JOURNAL OF MATERIALS SCIENCE 33 (1998) 2103–2109

EXAFS, magnetic, spectral, and thermal studies on a new polymeric copper mixed-valence compound with the 2-thioisoorotato bridging ligand

J. GARCÍA-RUIZ, J. BLASCO
Instituto de Ciencia de los Materiales de Aragón, C.S.I.C.-Universidad de Zaragoza, 50009 Zaragoza, Spain

F. HUESO-UREÑA, M. N. MORENO-CARRETERO*
Departamento de Química Inorgánica y Orgánica, Universidad de Jaén, 23071 Jaén, Spain
E-mail: mmororeno@ujaen.es

From the reaction, in aqueous medium, of 2-thioisoorotic acid and copper carbonate, an orange compound can be isolated. The formula unit contains only one copper and one 2-tioisoorotato anion. This compound has been studied by means of extended X-ray atomic force spectroscopy (EXAFS), magnetic measurements, spectral (infrared, electronic and electron paramagnetic resonance (EPR)) and thermal methods (thermogravimetry, differential scanning calorimetry, evolved gas infrared analysis). EXAFS measurements point out the existence of a first shell around the copper atoms formed by a sulphur atom (Cu–S 0.2209 nm) and two oxygen atoms (Cu–O 0.1947 nm). This coincides with the coordination mode proposed for the ligand from infrared data. The structure may be described as a chain-like structure in which the metal ions are bridged by 2-thioisoorotato anions through both oxygen atoms of the carboxylate group and the sulphur atom, (S2)]–Cu–[(O5,O5′)–2-thioisoorotato–(S2)]–Cu–[(O5,O5′). Also, the weak involvement of an endocyclic nitrogen atom in the four-membered chelate formation with the sulphur atom cannot be rejected except at distances Cu–N beyond 0.23 nm. Whereas EXAFS measurements detect the only presence of Cu(I), magnetic measurements indicate there is a mixture of valence states of copper atoms (10% Cu^{II} + 90% Cu^{I}). On the other hand, the compounds exhibit an axial EPR spectrum which is typical from a magnetically diluted Cu(II) compound with a stronger ligand field in the equatorial plane. Finally, in order to determine the homogeneity of this compound, we have analysed this sample by electron microscopy. It is composed of spheres with radii ranging between 1.3 and 1.7 μm and cylinders whose length ranges between 6 and 10 μm and width between 1.2 and 1.6 μm. Energy dispersive spectroscopic analysis was performed on several points and areas of this polymer. In all analyses, the ratio Cu : S was the expected 1 : 1 without any appreciable difference between spheres and cylinders. These results seem to indicate a similar composition in both morphologies, pointing to the presence of two polymorphic phases. This could be the reason for the unsuccessful attempts to obtain single crystals of this polymer to date.

1. Introduction

This paper is the last in a series reporting research focused on the structural study of metal complexes of isoorotic acid (5-carboxyuracil) derivatives. Thus, in the available literature, papers about thermal studies [1–4], spectral [5–7] and crystallographic studies [8–11] on isoorotic and 2-thioisoorotic ligands can be found. The biological importance of these organic molecules has been extensively pointed out in these articles. Many of the studied complexes display monomeric structures in which the organic ligand acts as a bidentate ligand through the exocyclic oxygen attached at the four position and one oxygen of the carboxylate group [9, 10]. However, there are some examples of tetrameric [11] or polymeric structures [6, 8] in which the isoorotato moiety acts as bridging ligand. This paper reports a wide study of the molecular structure of a polymeric copper complex with the 2-thioisoorotato ligand, $Cu(H_2CTU)$, in which +1 and +2 valence states for the metal ion seem to be mixed.

* Author to whom all correspondence should be addressed.

2. Experimental procedure

2.1. Synthesis

2-Thioisoorotic acid was purchased from Sigma and used without further purification. All the chemicals used in this work were analytical reagent grade. The synthesis of the complex was carried out by mixing 0.5 mmol copper(II) carbonate with 2 mmol 2-thioisoorotic acid in 200 ml hot water. The resulting suspension was stirred for a few hours and as a proportion of the metallic carbonate was digested, the colour changed from green to orange. When the total volume was reduced to around 50 ml, an orange-coloured powder was isolated. This was filtered off, washed with ethanol and diethylether and air-dried. In order to prevent the appearance of Cu(I)/Cu(II) mixtures, due to the great tendency of Cu(I) to oxidize to Cu(II), the same procedure was followed several times but using as copper compounds copper(I) chloride, copper(II) nitrate, and copper(II) sulphate, always with an amount of sodium sulphite in a slightly acid medium (to give a reducing atmosphere), which may help to obtain a pure Cu(I) complex. However, it must be pointed out that all experimental procedures lead to the same material being obtained. All attempts to obtain single crystals were unsuccessful. The analytical data (mean values from four different samples) were 25.23% C, 1.09% H, 12.07% N, 13.55% S. These data are in agreement with both $Cu^{I}C_5H_3N_2O_3S$ (25.59% C, 1.29% H, 11.94% N, 13.66% S) and $Cu^{II}C_5H_2N_2O_3S$ (25.70% C, 0.86% H, 11.99% N, 13.72% S) formulas. Experimental data reported in this paper indicate that this compound contains *ca.* 10% Cu(II) and *ca.* 90% Cu(I) (referred to total copper). Also, a 0.003% volume of ferromagnetic spureous impurities has been detected. For this reason, the complex has been named $Cu(H_2CTU)$, in which the only presence of Cu(I) is supposed.

2.2. Apparatus and methods

Microanalyses of carbon, hydrogen and nitrogen were performed in the Technical Services of the University of Granada (STUGRA). Thermogravimetric studies were carried out under pure air (150 ml min^{-1}) on a Shimadzu TGA-50H thermobalance provided with a FT–IR Nicolet-510 apparatus for the evolved gas analysis, using 11.48 mg sample and a 5 °C min^{-1} heating rate. The differential scanning calorimetry (DSC) plot was recorded on a Mettler DSC-20 (static air atmosphere, 1.95 mg sample, 5 °C min^{-1} heating rate) and a Shimadzu DSC-50 machine (nitrogen atmosphere 50 ml min^{-1}, 1.45 mg sample, 10 °C min^{-1} heating rate). Infrared spectra were obtained on a Perkin–Elmer FT–IR 1760X (KBr pellets, 4000–400 cm^{-1}) and a Perkin–Elmer 983G spectrometer (polyethylene pellets, 600–180 cm^{-1}). The EPR spectrum was obtained in the X-band at 153 K on a Varian E-109 apparatus, with a microwave frequency of 8.974 GHz and a modulation frequency of 100 kHz. The reflectance diffuse spectrum (240–1500 nm) was recorded on a Shimadzu MPC-3100 machine using, as reference, a $BaSO_4$ pellet. X-ray absorption spectra at the Cu*K* edge of $Cu(H_2CTU)$ were performed at the Synchrotron Radiation Source of the Daresbury Laboratory (UK), the storage ring operating at 2 GeV with a beam current of approximately 150 mA. The radiation was monochromatized using a double Si (1 1 1) crystal and harmonics rejection was performed by slightly detuning the two crystals. The absorption spectra were recorded in the transmission mode at room temperature. The samples for extended X-ray atomic force spectroscopy (EXAFS) measurements were prepared by spreading the powder on a Kapton tape and the thickness was optimized by adding further Kapton layers while checking the absorption edge step. The samples *bis*-thiourea-copper(I) chloride [18], *bis*(6-amino-1,3-dimethyl-5-nitrosouracilato-N5,N6) diaqua copper(II) [19] and *bis*(1,3-dimethyl-violurato-N5,O4) diaqua copper(II) [20] (denoted by $Cu(tu)_2Cl$, $Cu(DANU)_2(H_2O)_2$ and $Cu(DMV)_2(H_2O)_2$, respectively) were also measured and used as model spectra.

D.c. magnetization and a.c. susceptibility measurements were done using a Quantum Design (SQUID) magnetometer.

Transmission electron microscopy measurements of $Cu(H_2CTU)$ were carried out in a Jeol JSM-6400 with an electron beam of 20 keV. Elemental analysis was performed by energy dispersive X-ray analysis (EDX) of Link Analytical using a Si(Li) detector.

3. Results and discussion

3.1. Thermal analysis

Thermogravimetric data of this compound indicate that it is thermally stable for temperatures up to 300 °C. At this temperature, an abrupt decomposition process starts, which is reflected in the differential scanning calorimetry (DSC) plot by the appearance of an exothermic peak at 370 °C (air atmosphere) and the corresponding endothermic peak at 362 °C (nitrogen atmosphere). Infrared data of the evolved gas clearly show that the decomposition products of this weight-loss step are carbon dioxide, sulphur dioxide and nitrogen oxides. The infrared spectrum of the remaining product, which is stable between 400 and 620 °C, corresponds to $Cu_3(OH)_4(SO_4)$ [12, 13] (experimental weight loss 50.99%, calculated 49.61%). At 620 °C, there is a second weight loss which finishes at 770 °C. The evolved gas infrared analysis (EGA-IR) indicates that only H_2O and SO_2 are the gaseous products of this second step, which arise from the dehydration and decomposition of the copper(II) hydroxysulphate to give CuO as final residue; this also confirms that all the nitrogen is lost in the first weight-loss effect. Despite the experimental weight loss for this process (17.69%) being in agreement with that calculated if CuO becomes the only residue (16.49%), the infrared spectrum of the remaining material indicates there is a small amount of copper sulphate together with the copper oxide.

3.2. Infrared spectra

The infrared spectrum of the compound shows bands assignable [2] to ν(N–H) and ν(C–H)

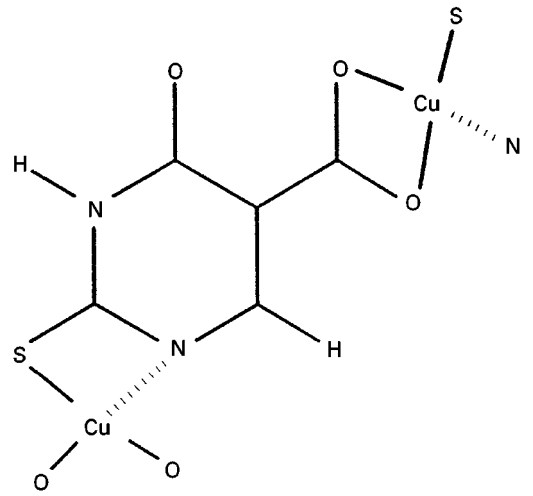

Figure 1 Polymeric structure proposed from infrared data. The primary coordination shell of metal ion coincides with the EXAFS results. Although N1-chelation is depicted, it is only tentative, and may be also N3-chelation.

(3300–2400 cm^{-1}), ν(C=O) (1705 cm^{-1}), ν(C=C) (1608 cm^{-1}), ν(NCS) (1526 cm^{-1}, thioamide I), ν(NCS) + ν(CS) (1162 cm^{-1}, thioamide III) and $\nu_{sym}(COO^-)$ (1448 cm^{-1}). The position of this last band strongly suggests that the carboxylate group acts as bidentate ligand [14], whereas the carbonyl group does not seem to be involved in the coordination, because the ν(C=O) band is only slightly shifted to the upper wave number if compared with the infrared spectra of sodium and ammonium salts (1699 and 1701 cm^{-1}, respectively) [2]. Also, upon coordination, the bands assigned to thioamide I and III are displaced from their position in the above-cited salts spectra, which may be indicative of the existence of a metal–sulphur bond. From these data, a coordination scheme in which the 2-thioisoorotato ligand acts as a bridging ligand between two metal centres with a four-membered (O5,O5′) chelate formation with one metal ion and one metal–sulphur bond with the other metal ion [8]. However, the changes detected in the thioamide bands may also suggest that the metal–sulphur bond is reinforced with a four-membered chelate formation with a neighbour endocyclic nitrogen atom. The far-infrared spectrum does not allow the suggestion of any band corresponding to metal–ligand vibrations. From these data, a polymeric (S2)]–Cu–[(O5,O5′)–2-thioisoorotato–(S2)]–Cu–[(O5,O5′) structure, as depicted in Fig. 1, may be proposed, which is coincident with results obtained from extended X-ray atomic force spectroscopy (EXAFS) measurements.

3.3. EXAFS measurements

The experimental EXAFS signal has been extracted from the raw spectra following standard methods [15]. Background removal was performed and the atomic absorption coefficient was determined by a low-order polynomial fit of the spectrum.

The EXAFS spectra and their Fourier transform (FT), performed 25 and 115 nm^{-1} using a gaussian

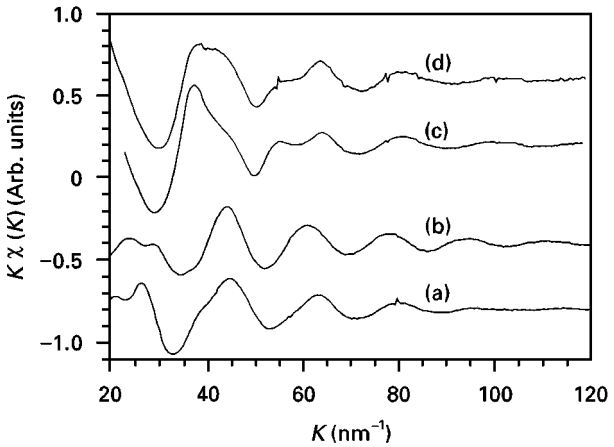

Figure 2 Cu*K*-edge EXAFS spectra of (a) $Cu(H_2CTU)$, (b) $Cu(tu)_2Cl$, (c) $Cu(DMV)_2(H_2O)_2$ and (d) $Cu(DANU)_2(H_2O)_2$ samples.

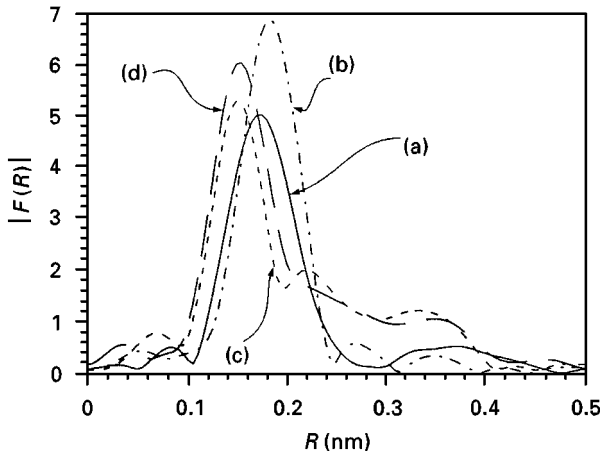

Figure 3 Comparison of the $k^3\chi(k)$ Fourier transform of (a) $Cu(H_2CTU)$, (b) $Cu(tu)_2Cl$, (c) $Cu(DMV)_2(H_2O)_2$ and (d) $Cu(DANU)_2(H_2O)_2$ samples.

window, of *bis*-thiourea-copper(I) chloride, *bis*(6-amino-1,3-dimethyl-5-nitrosouracilato-N5,N6)diaqua copper(II), *bis*(1,3-dimethyl-violurato-N5,O4)-diaqua copper(II) (denoted $Cu(tu)_2Cl$, $Cu(DANU)_2(H_2O)_2$ and $Cu(DMV)_2(H_2O)_2$, respectively) and $Cu(H_2CTU)$ samples are shown in Figs 2 and 3, respectively. The EXAFS spectrum of the 2-thioisoorotato complex shows a nearly single frequency oscillation which indicates that contributions beyond the first shell interfere in a destructive way. The same effect occurs for the $Cu(tu)_2Cl$ sample. As expected, the FT of our problem shows a unique peak at $R = 0.173$ nm (peak position is not corrected for the atomic phase shift and, consequently, does not correspond to real interatomic distances) corresponding to the first coordination shell of copper. The other samples also show a main peak at $R = 0.153$ nm $(Cu(DANU)_2(H_2O)_2$ and $Cu(DMV)_2(H_2O_2)$ and $R = 0.185$ nm $(Cu(tu)_2Cl)$. Owing to the lack of contributions at high frequencies, we restricted our study to the copper first coordination shell.

The first shell contribution was extracted by Fourier filtering of the spectra in the following conditions: between 0.100 and 0.195 nm for

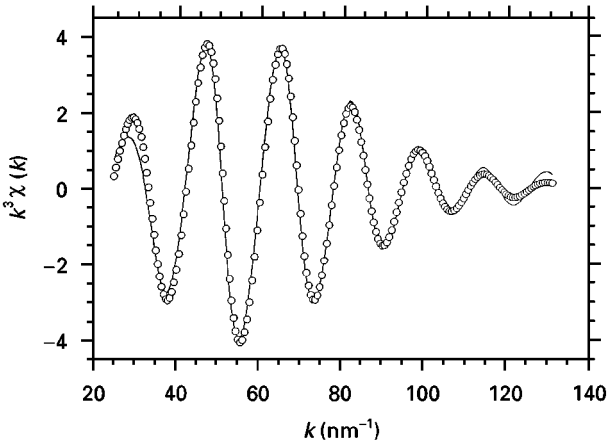

Figure 4 (○) Experimental and (—) best fit of the k^3-weighted filtered EXAFS signal of the first shell of the Cu(H_2CTU) sample.

TABLE I Best fit parameters obtained from the first shell contribution and absorption edges for the analysed samples (*n*, coordination number; *R*, distance from the copper adsorber; σ, Debye–Waller factor)

Sample		*n*	*R*(nm)	σ(10^{-3} nm^2)	E_0(eV)
Cu(H_2CTU)	Cu–O	2	0.1947	0.16	8978.5
	Cu–S	1	0.2209	0.10	
Cu(tu)$_2$Cl	Cu–S	3	0.2233	0.14	8978.5
Cu(DANU)$_2$(H_2O)$_2$	Cu–N	4	0.1960	0.10	8985.9
Cu(DMV)$_2$(H_2O)$_2$	Cu–N	2	0.1927	0.04	8986.8
	Cu–O	2	0.2012	0.08	

Cu(DANU)$_2$(H_2O)$_2$ and Cu(DMV)$_2$(H_2O)$_2$, between 0.110 and 0.225 nm for Cu(tu)$_2$Cl and Cu(H_2CTU) samples. The structural parameters were obtained by least-square fitting of the Fourier-filtered EXAFS signal to the EXAFS formula [16] using the EXCURV package program [17]. In Fig. 4, the EXAFS signal and FT of this shell for Cu(H_2CTU) sample together with the obtained best fits are shown. The results of the fits are summarized in Table I.

The coordination number and interatomic distances for reference samples Cu(tu)$_2$Cl, Cu(DANU)$_2$(H_2O)$_2$ and Cu(DMV)$_2$(H_2O)$_2$ agree quite well with the crystallographic data reported elsewhere [18–20] and it is a probe of the accuracy of the analysis method. Note that in Cu/DMV and Cu/DANU compounds, the copper atoms have a six-coordination shell but they show a high Jahn–Teller effect resulting in an effective 4 + 2 coordination and, in our measurements, the larger Cu–O distances (*ca.* 0.23 nm, from coordinated water [19, 20]) get together to form a second coordination shell.

The main result we have obtained is a coordination number of 3 for the metallic atom in the Cu(H_2CTU) sample, similar to that reported for Cu(tu)$_2$Cl [18]. Nevertheless, in this sample, the first shell is formed by two oxygens at 0.1947 nm and one sulphur at 0.2209 nm. The fourth coordination of the copper atom could be a nitrogen atom of the neighbour cycle but at distances above 0.23 nm.

Other useful information we have obtained is the valence state of the copper by comparing the chemical shift of the absorption edge energy. We have estimated the energy of the absorption threshold in the different samples by the maximum of the derivative at the edge (inflexion point). In Table I, the photoionization energies of the different compounds are compared. From these values, the chemical shift in the absorption spectra edge between Cu(I) and Cu(II) can be estimated to be around 7.4–8.3 eV. The absorption edge of the Cu(H_2CTU) complex is equal to that corresponding to the copper–thiourea complex [18] and is shifted from the other two samples by about 8 eV, showing that the copper atom is in the +1oxidation state.

3.4. Electronic and electron paramagnetic resonance (EPR) spectra

In addition to the ligand's bands, the UV–VIS–NIR reflectance diffuse spectrum of this compound displays two bands at 20 100 and 13 700 cm^{-1}. The first band, five times more intense than the second, may be assigned to a ligand to metal charge transfer between occupied sulphur orbitals (probably of σ type) and available Cu(II) orbitals (probably d_{x2-y2}) [21]. The second band, very weak and broad, corresponds to the sum of various *d–d* transitions that may take place in either a roughly square-planar or tetragonally-distorted Cu(II) ion [21].

The powder EPR spectrum (Fig. 5) is an axial spectrum with $g_{\parallel} = 2.24$ and $g_{\perp} = 2.05$ in which hyperfine structure can be observed. This fact is due to the presence of diluted Cu(II) centres and is in agreement with the presence of a polymer in which only a small amount of copper atoms are in the +2 oxidation state, the others displaying the +1 oxidation state [22]. The value of $G = 4.8$ indicates that the local tetragonal axes are aligned parallel or only slightly misaligned and there is no exchange coupling between Cu(II) ions [23]. Also, as pointed out by some authors [24, 25], the large separation between the hyperfine structure signals ($A_{\parallel} = 200$ mT) may be taken as a measure of the higher strength of the in-plane ligand field under tetragonal geometry in Cu(II) complexes.

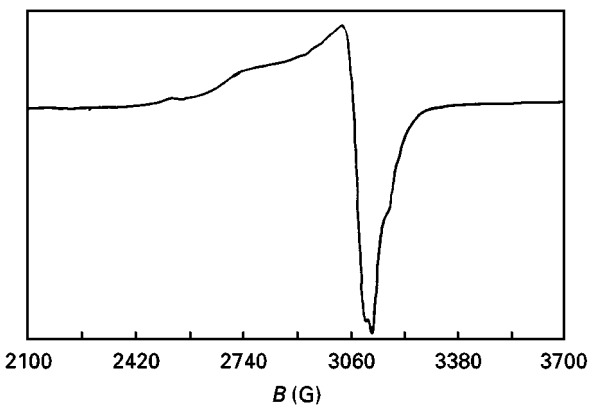

Figure 5 EPR powder spectrum of Cu(H_2CTU) at 153 K.

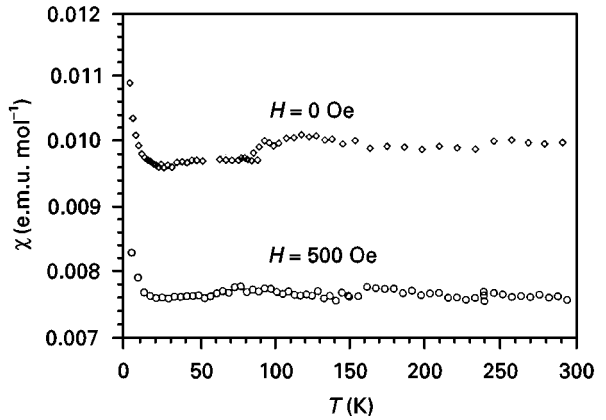

Figure 6 Comparison of the a.c. magnetic susceptibility of $Cu(H_2CTU)$ sample without and with a d.c. external magnetic field (500 Oe).

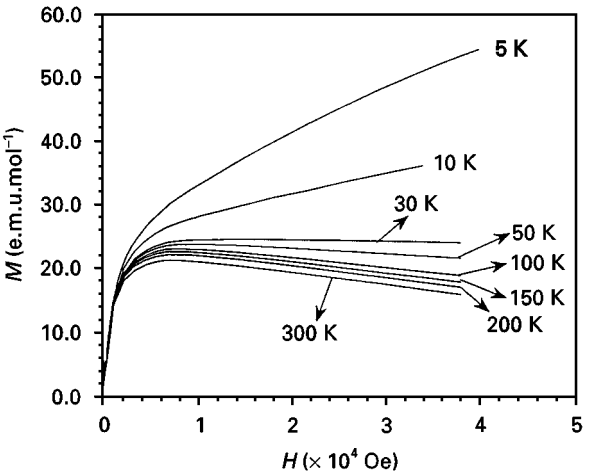

Figure 8 Isotherms of magnetization increasing the magnetic field for $Cu(H_2CTU)$ sample. The temperature is given for each curve.

3.5. Magnetic measurements

Fig. 6 shows the a.c. magnetic susceptibility from 5 K up to 300 K for $Cu(H_2CTU)$ sample. The a.c. susceptibility was measured under two conditions, with an external d.c. magnetic field of 500 G and without external magnetic field. Both measures show an identical behaviour as can be seen in Fig. 6. For temperatures higher than 20 K, the susceptibility is independent of temperature while a rise in the paramagnetic signal is observed at lower temperatures. The main difference in both curves arises from the magnitude of the paramagnetic signal, more than 100% higher for the measurement without an external field. This is an indication of a strong dependence of the susceptibility with the external magnetic field characteristic of ferromagnetic interactions.

In Fig. 7, the d.c. magnetization of the same sample in the $5\,K < T < 300\,K$ range can be seen. This curve also shows two different regions with a change in the slope, around 20 K, of the magnetization from negative ($T < 20$ K) to positive ($T > 20$ K). The slight increase of the magnetization with temperature in the second region indicates weak ferromagnetic interactions.

In order to clarify the magnetic behaviour of this sample, we have carried out magnetization, M, versus magnetic field, H, isotherms at different temperatures (5, 10, 30, 50, 100, 150, 200, 240, 280, and 300 K). As may be observed from Fig. 8, the magnetic behaviour of this material is complicated but clearly explains the difference between the susceptibility at zero field and the susceptibility at 500 G due to the lack of linearity of the magnetization curves. The main points to be stressed in this behaviour are as follows: (i) the sample shows magnetic saturation at around 6500 G external magnetic field over the whole temperature range; (ii) at higher fields, the magnetization shows a linear dependence with a positive slope for low temperatures (5 and 10 K) and a negative slope at higher temperatures.

This behaviour can be explained as due to the addition of three contributions: a ferromagnetic contribution which saturates at relatively low field, a positive paramagnetic contribution (linear dependence with positive slope at low temperatures) and a diamagnetic contribution (linear dependence with constant negative slope at high temperatures). At low temperatures, the preponderance of a paramagnetic signal versus the diamagnetic one gives rise to a positive slope in the magnetization curve. On the contrary, at high temperatures, the diamagnetic contribution of core ions shadow the paramagnetic one.

The magnetization of saturation at 0 K and zero field has been obtained using the well-known law

$$\frac{M_{(H=0,T)}}{M_{(H=0,T=0)}} = C^{3/2}\,T^{3/2} \qquad (1)$$

In Fig. 9, the plot of $M_{(H=0,T)}$ versus $T^{3/2}$ giving a linear dependence is shown. $M_{(H=0,T)}$ is obtained by extrapolating the linear region of Fig. 8 down to zero field. Extrapolating the line of Fig. 9 down to $T = 0$ K, an $M_{(H=0,T=0)}$ value of 25.4 e.m.u. mol^{-1} has been obtained. This magnetization of saturation corresponds to a $\mu_{ef} = 0.0045$ BM. We assign the origin of this low magnetization to spureous magnetic impurities instead of a weak internal ferromagnetism.

In order to obtain a rough approximation of the other magnetic contributions, we have plotted the slope of the linear region of Fig. 8 versus temperature

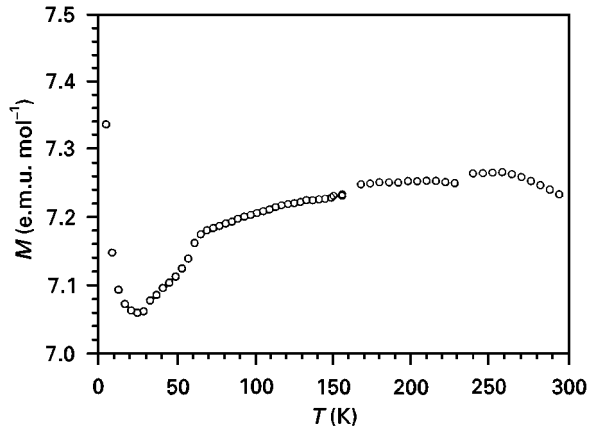

Figure 7 D.c. magnetization with external field of 500 Oe for $Cu(H_2CTU)$ sample.

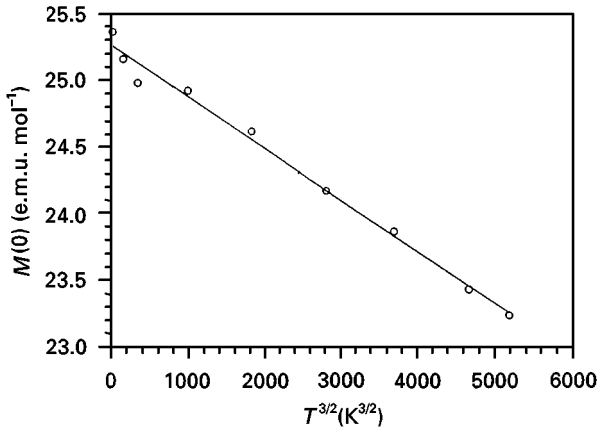

Figure 9 Magnetization of saturation ($H = 0$) versus $T^{3/2}$ for $Cu(H_2CTU)$ sample.

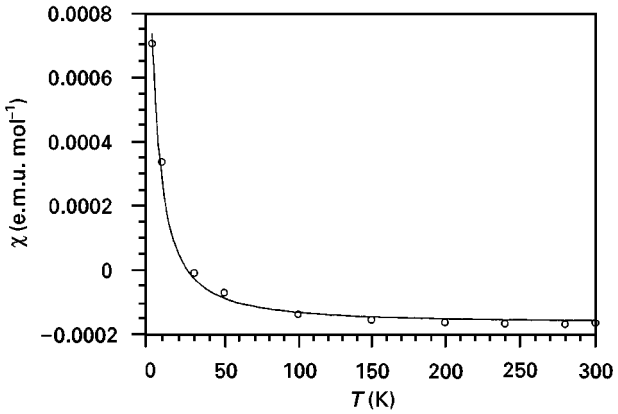

Figure 10 Extrapolated d.c. magnetic susceptibility (see text) versus temperature for $Cu(H_2CTU)$ sample.

after substracting the diamagnetic signal of the sample holder (2×10^{-8} e.m.u.). The result can be seen in Fig. 10, where a Curie-like curve has been obtained. This curve has been fitted to the law

$$\chi = \frac{C}{T} + \chi_0 \qquad (2)$$

The fit gives the values of $C = 4.36\,\text{e.m.u.}\,\text{K}^{-1}\,\text{mol}^{-1}$ and $\chi_0 = -1.1 \times 10^{-4}\,\text{e.m.u.}\,\text{mol}^{-1}$. The parameter χ_0 is related with the core diamagnetism neglecting further contributions such as Van-Vleck or Pauli paramagnetism, and agrees quite well with that expected for $Cu(H_2CTU)$ ($-0.97 \times 10^{-4}\,\text{e.m.u.}\,\text{mol}^{-1}$). On the other hand, the paramagnetic effective moment obtained per unit formula is 0.18 BM. This result indicates the presence of a minor paramagnetic phase together the ferromagnetic impurities and a main diamagnetic phase. Considering an ion of $S = 1/2\,(Cu^{2+})$, the amount of different phases can be estimated as follows: paramagnetic phase around 8%–10% (in volume), 0.003% ferromagnetic impurities, and the rest (around 90%) must be the diamagnetic phase. This result agrees with a main diamagnetic phase with Cu^{+}, as can be inferred from the EXAFS results, together with minor phases with Cu^{2+}, which are responsible for the EPR signal detected in the sample.

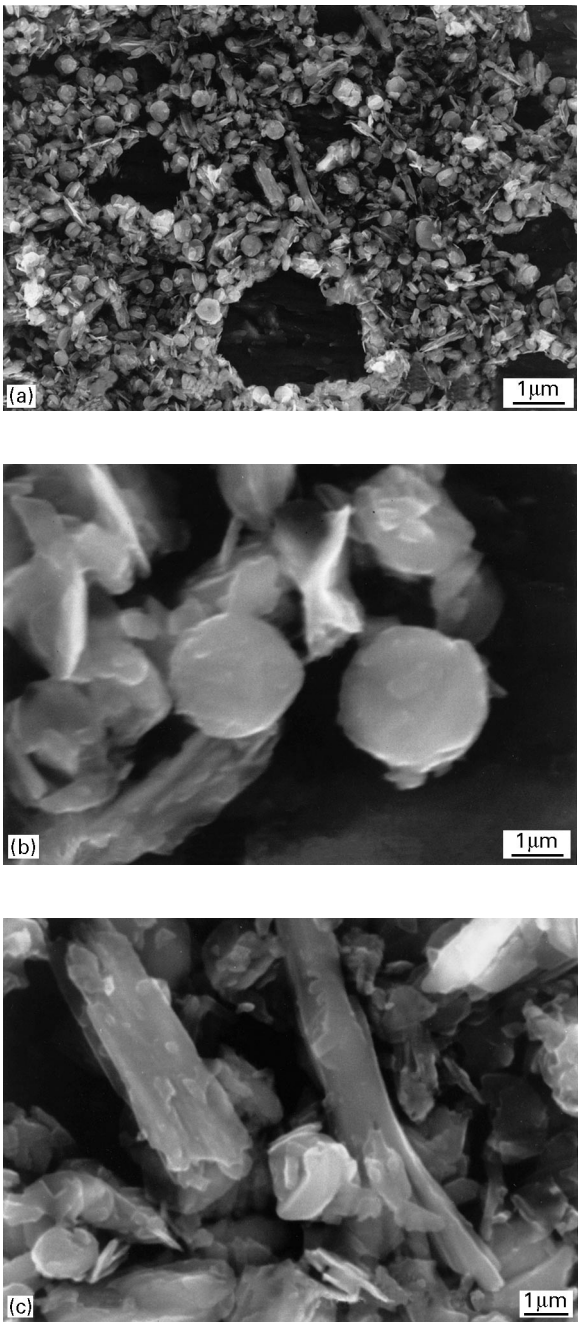

Figure 11 Scanning electron micrographs from $Cu(H_2CTU)$ sample: (a) a general overview; (b) detail of spheres; (c) detail of cylinders.

3.6. Transmission electron microscopy

In order to determine the homogeneity of this compound and to detect the kind of impurities detected by magnetic measurements, we have analysed this sample by electron microscopy. In Fig. 11a, an overview of the microstructural features of this compound is shown. It is composed of spheres with radii ranging between 1.3 and 1.7 μm and cylinders whose length ranges between 6 and 10 μm and the width between 1.2 and 1.6 μm. In Fig. 11b and c, more detailed scanning electron micrographs of both kinds of morphology are shown.

EDS analysis was performed on several points and areas of this polymer. In all analyses, the ratio Cu:S was the expected 1:1 without any appreciable difference between spheres and cylinders. These results seem to indicate a similar composition in both

morphologies pointing to the presence of two polymorphic phases. This could be the reason for the unsuccessful attempts to obtain single crystals of this polymer to date.

Acknowledgements

Thanks are due to Professors A. Rodríguez González-Elipe and E. Colacio-Rodríguez for their kind advice.

References

1. F. HUESO-UREÑA, M. N. MORENO-CARRETERO, J. M. SALAS-PEREGRÍN, C. VALENZUELA-CALAHORRO and G. ALVAREZ DE CIENFUEGOS-LOPEZ, *Thermochim Acta* **133** (1988) 341.
2. F. HUESO-UREÑA, M. N. MORENO-CARRETERO and J. M. SALAS-PEREGRÍN, *ibid.* **170** (1990) 225.
3. F. HUESO-UREÑA, M. N. MORENO-CARRETERO, J. M. SALAS-PEREGRÍN and M. A. ROMERO-MOLINA, *ibid.* **177** (1991) 119.
4. F. HUESO-UREÑA and M. N. MORENO-CARRETERO, *ibid.* **182** (1991) 9.
5. B. E. DOODY, E. R. TUCCI, R. SCRUGGS and N. C. LI, *J. Inorg. Nucl. Chem.* **28** (1966) 833.
6. F. HUESO-UREÑA, M. N. MORENO-CARRETERO, J. M. SALAS-PEREGRÍN and G. ALVAREZ DE CIENFUEGOS-LOPEZ, *J. Inorg. Biochem.* **43** (1991) 17.
7. G. MAISTRALIS, N. KATSAROS, S. P. PERLEPES and D. KOVALA-DEMERTZI, *ibid.* **45** (1992) 1.
8. F. HUESO-UREÑA, M. N. MORENO-CARRETERO, J. M. SALAS-PEREGRÍN and G. ALVAREZ DE CIENFUEGOS-LOPEZ, *Trans. Metal Chem.* **20** (1995) 262.
9. G. MAISTRALIS, N. KATSAROS, D. MENTZAFOS and A. TERZIS, *Acta Crystallogr.* **C47** (1991) 740.
10. F. HUESO-UREÑA, M. N. MORENO-CARRETERO, M. A. ROMERO-MOLINA, J. M. SALAS-PEREGRIN, M. P. SÁNCHEZ-SÁNCHEZ, G. ALVAREZ DE CIENFUEGOS-LOPEZ and R. FAURE, *J. Inorg. Biochem.* **51** (1993) 613.
11. F. HUESO-UREÑA, M. N. MORENO-CARRETERO, M. QUIRÓS-OLOZÁBAL, J. M. SALAS-PEREGRÍN, R. FAURE and G. ALVAREZ DE CIENFUEGOS-LÓPEZ, *Inorg. Chim. Acta* **241** (1995) 61.
12. E. A. SECCO, *Can. J. Chem.* **66** (1988) 329.
13. *Idem*, *ibid.* **66** (1988) 337.
14. K. NAKAMOTO, in "Infrared and Raman Spectra of Inorganic and Coordination Compounds", 4th Edn (Wiley, New York, 1986).
15. D. C. KONINGSBERGER and R. PRINS, in "X-ray Absorption: Principles, Applications, Technique of EXAFS, SEXAFS and XANES" (Wiley, New York, 1988).
16. M. C. SANCHEZ-SIERRA, J. GARCÍA-RUIZ, M. G. PROIETTI and J. BLASCO, *J. Mol. Cat.* **A96** (1995) 65.
17. N. BINSTED, S. J. GURMAN and Y. CAMPBELL, in "EXCURV88 program" (SERC Daresbury Laboratory).
18. W. A. SPOFFORD and E. L. AMMA, *Acta Crystallogr.* **B26** (1970) 1474.
19. J. M. SALAS-PEREGRÍN, M. A. ROMERO-MOLINA, M. P. SÁNCHEZ-SÁNCHEZ, M. N. MORENO-CARRETERO, M. QUIRÓS-OLOZÁBAL and R. FAURE, *Polyhedron* **11** (1992) 2217.
20. M. A. ROMERO-MOLINA, J. D. MARTÍN-RAMOS, J. D. LÓPEZ-GONZÁLEZ and C. VALENZUELA-CALAHORRO, *Ann. Quím.* **79B** (1983) 200.
21. A. B. P. LEVER, in "Inorganic Electronic Spectroscopy", 2nd Edn (Elsevier, Amsterdam, 1984).
22. J. R. PILBROW, in "Transition Ion Electron Paramagnetic Resonance" (Oxford Science, Oxford, 1990).
23. B. J. HATHAWAY and D. E. BILLING, *Coord. Chem. Rev.* **5** (1970) 143.
24. A. S. BRILL, *Molec. Biol. Biochem. Biophys.* **26** (1977) 43.
25. J. M. MORENO, J. RUIZ, J. M. DOMÍNGUEZ-VERA, E. COLACIO, D. GALISTEO and R. KIVËKAS, *Polyhedron* **13** (1994) 203.

Received 9 December 1996
and accepted 27 November 1997